



**HAL**  
open science

## Urban mining of unexploited spent critical metals from E-waste made possible using advanced sorting

Nicolas Charpentier, Ange Maurice, Dong Xia, Wen-Jie Li, Chang-Sian Chua,  
Andrea Brambilla, Jean-Christophe P. Gabriel

### ► To cite this version:

Nicolas Charpentier, Ange Maurice, Dong Xia, Wen-Jie Li, Chang-Sian Chua, et al.. Urban mining of unexploited spent critical metals from E-waste made possible using advanced sorting. *Resources, Conservation and Recycling*, 2023, 196, pp.107033. 10.1016/j.resconrec.2023.107033 . hal-04095661

**HAL Id: hal-04095661**

**<https://hal.science/hal-04095661>**

Submitted on 12 May 2023

**HAL** is a multi-disciplinary open access archive for the deposit and dissemination of scientific research documents, whether they are published or not. The documents may come from teaching and research institutions in France or abroad, or from public or private research centers.

L'archive ouverte pluridisciplinaire **HAL**, est destinée au dépôt et à la diffusion de documents scientifiques de niveau recherche, publiés ou non, émanant des établissements d'enseignement et de recherche français ou étrangers, des laboratoires publics ou privés.

# Urban Mining of Unexploited Spent Critical Metals from E-waste Made Possible Using Advanced Sorting

Nicolas M. Charpentier<sup>1,2,\*</sup>, Ange A. Maurice<sup>1</sup>, Dong Xia<sup>1</sup>, Wen-Jie Li<sup>3</sup>, Chang-Sian Chua<sup>3</sup>, Andrea Brambilla<sup>4</sup>, Jean-Christophe P. Gabriel<sup>1,2,\*</sup>

<sup>1</sup> SCARCE Laboratory, Energy Research Institute @ NTU (ERI@N), Nanyang Technology University, 637553, Singapore.

<sup>2</sup> Université Paris-Saclay, CEA, CNRS, NIMBE, LICSEN, 91191, Gif-sur-Yvette, France.

<sup>3</sup> School of Material Science and Engineering, Nanyang Technology University, 639798, Singapore.

<sup>4</sup> Université Grenoble Alpes, CEA Leti, 38054 Grenoble, France

\* Corresponding authors: NM Charpentier (nicolas.charpentier2@cea.fr), JCP Gabriel (jean-christophe.gabriel@cea.fr)

**KEYWORDS:** Recycling, Waste PCBs, computer vision, Multi-energy X-ray Transmission, hyperspectral imaging, waste management

## Abstract

The growing number of electronic devices has led to a surge in e-waste, making efficient recycling essential to reduce environmental impact and recover valuable metals. However, traditional recycling methods struggle to extract them due to their low concentrations in e-waste. Here, we developed a system to sort electronic components from printed circuit boards by elemental composition. It combines a convolutional neural network-based optical recognition with multi-energy X-ray transmission spectroscopy, demonstrating up to 96.9% accuracy in controlled conditions. Hence, with elemental enrichments by up to 10,000 for targeted elements, this method renders economically viable the recovery of previously unrecycled critical metals by enriching sorting bags in precious, semi-precious, refractory (Ta, Nb), transition (Co, Cr, Mn, Ni, Zn, Ga, Bi, etc.) or other (In, Sn, Sb) metals. These findings demonstrate the promising applications of this technology in mitigating the environmental impact of e-waste and promoting the sustainable recovery of valuable metals.

## 1. INTRODUCTION

The technological development and the automation of our modern society is supported by an exponential increase in our use of electronics, which leads to a similar increase in the amount of waste from electrical and electronic equipment (WEEE) (Forti et al. 2020). Manufacturing these devices requires a considerable volume of raw materials including valuable ones (gold, palladium, silver...), critical elements (rare earth

elements (REEs) (Binnemans, McGuinness, and Jones 2021), tantalum, cobalt...) as well as hazardous products (lead, chromium, bromine...) (Wang and Xu 2015). Thus, making the electronic industry (considered from cradle to cradle) one of the most environmentally impacting (Shakil, Nawaz, and Sadeef 2023).

A good way to reduce this industry's footprint would be to increase the efficiency of its recycling processes. But

1 for this to happen, the major issue of the  
2 elemental complexity of the WEEEs'  
3 composition needs to be addressed. On  
4 that front, printed circuit boards (PCBs)  
5 (Gorewoda et al. 2020), hold the record  
6 with more than sixty chemical elements  
7 that can be found in them (Maurice et al.  
8 2021). Current methods of treating waste  
9 PCBs (WPCBs), which consist in first  
10 crushing and grinding them, produce a  
11 powder with a highly complex and  
12 heterogeneous chemical composition. This  
13 is then followed by physical separation of  
14 some particles (Kaya 2017) and the  
15 subsequent pyrometallurgical and  
16 hydrometallurgical process steps. With  
17 such an approach, although 60% of the  
18 value can be retrieved from the WPCBs, it  
19 only recycles one quarter of the chemical  
20 elements it contains, either the most  
21 concentrated or the most valuable (C, Cu,  
22 Ni, Fe, Al, Ti, Cr, Au, Pt, Ag, Pd, Pb, Sn)  
23 (Wu et al. 2017). Indeed, with such  
24 processing, most other elements of interest  
25 become too diluted in the overall waste  
26 (down to a few ppm levels) and are  
27 therefore impossible to extract in an  
28 economically viable way. These elements  
29 are therefore lost as ash and disposed of  
30 through landfilling (U.S. Environmental  
31 Protection Agency and Conservation  
32 2020).

33 To more effectively access these spent  
34 chemical elements an alternative strategy  
35 is to dismantle WPCBs to recover the  
36 electronic components (ECs) and sort  
37 them according to their type and chemical  
38 composition (Maurice et al. 2021). Recent  
39 studies have therefore explored some  
40 possible electronic components sorting  
41 and subsequent refining processes, such as  
42 optical sorting based on machine vision  
43 coupled with artificial intelligence (for  
44 example, convolutional neural network -  
45 CNN). The latter has shown promising  
46 results for the classification of ECs

47 (Lefkaditis and Tsirigotis 2010; Lu et al.  
48 2022). So far, these methods have been  
49 limited to only a few EC categories,  
50 giving access to only a few more chemical  
51 elements. Other processes have privileged  
52 a selective robotic disassembly (pick and  
53 choose approach), which requires high  
54 precision for removing the targeted ECs.  
55 However, with a speed of a few tenths of a  
56 second per component retrieved, it can  
57 only be applied to high value ECs to be  
58 economically viable (Sauer et al. 2019).  
59 However, despite the significant  
60 improvement that these recent innovations  
61 have brought, these EC sorting techniques  
62 all rely on optical recognition, which has  
63 its own limitations. Indeed, while it is  
64 effective when components looking alike  
65 have similar composition (Kopacek 2016),  
66 it does not allow for elemental separation  
67 when components look similar but have  
68 different chemical compositions.  
69 Moreover, the elemental composition of  
70 PCBs can vary significantly due to their  
71 diverse origins, as highlighted by previous  
72 studies (Smalcerz et al. 2023). For  
73 example, this is observed with capacitors,  
74 multilayer ceramic capacitors or resistors.  
75 To tackle this issue, various spectroscopic  
76 methods have been developed such as  
77 near infrared (NIR) hyperspectral image  
78 spectroscopy (HSI) (Rapolti et al. 2021)  
79 or laser-induced breakdown spectroscopy  
80 (LIBS) (Zeng et al. 2021) giving access to  
81 some elemental composition of the  
82 components' surfaces. Using either  
83 spectra analysis or artificial intelligence  
84 these methods have shown high accuracy  
85 in the targeting of specific elements. Other  
86 recent studies have showed great  
87 progresses in the recognition of e-waste  
88 parts by combing optical imaging and HSI  
89 (Tan et al. 2022). However, all these  
90 approaches can only analyse the surface  
91 composition of ECs and do not capture all  
92 the internal chemical composition and  
93 elements. For this reason, these are useful

1 methods for the characterisation and  
2 sorting of homogeneous or monolithic  
3 materials such as plastics. To get access to  
4 some internal composition indication, few  
5 energies (one to five) X-ray transmission  
6 (XRT) spectroscopies have been used in a  
7 variety of fields such as mining (Veras et  
8 al. 2020; Yeyu et al. 2021), food industry,  
9 medical imaging (Mesina, de Jong, and  
10 Dalmijn 2007) or even plastic waste  
11 sorting (Hennebert and Filella 2018), but  
12 these approaches do not have enough  
13 energy resolution to allow for the  
14 elemental sorting of mixture as complex  
15 as wasted electronic components from  
16 WPCBs. Hence, this study where we  
17 present a novel sorting method for ECs  
18 using both optical and Multi-Energy XRT  
19 (MEXRT) sorting (up to 128 energy  
20 levels) in which ECs were sorted on a  
21 custom-made prototype using a CNN for  
22 image recognition followed by MEXRT  
23 hyperspectral image spectroscopy  
24 analysis. We will show that it allows for  
25 the accurate classification of ECs based on  
26 their type and elemental composition  
27 leading to such an enrichment in many  
28 targeted elements, so as to provide access  
29 to previously unrecoverable spent  
30 elements.

## 31 **2. MATERIALS AND METHODS**

### 32 **2.1. Materials**

33 For this study, model ECs from various  
34 manufacturers, with known specifications,  
35 were purchased from the distributor RS  
36 Components Singapore. They were then  
37 mixed with other ECs retrieved from the  
38 disassembly of spent printed circuit  
39 boards of various origins to form the  
40 model samples for the study. These PCBs,  
41 were extracted from end-of-life electronic  
42 products, from various applications such  
43 as mobile phones, domestic appliances,  
44 computers, or industrial devices, by  
45 manually dismantling the appliances.

46 These PCBs were then disassembled by  
47 heating them in a furnace at ~200 °C for  
48 10 minutes, to melt the solder, before  
49 being manually shaken or hammered to  
50 release and collect loose spent ECs. The  
51 latter were used to form the initial e-waste  
52 stream for the large-scale study.

53 Nitric acid (AR, 70 %), hydrochloric acid  
54 (AR, 37 %), and hydrogen peroxide  
55 solution (3 %), were purchased from  
56 Sigma-Aldrich. Metal standard solutions  
57 for ICP were purchased from PerkinElmer.  
58 Ultra-pure water was obtained from a  
59 water purification system (WaterPro®,  
60 Labconco Co.) with a resistivity of  
61 18.2 MΩ·cm at 25 °C. All the chemicals  
62 were used as received.

### 63 **2.2. Sieving**

64 Once disassembled from the boards, ECs  
65 were segregated into 5 size categories by  
66 sieving. Using Retsch AS 300 shaker with  
67 screens of 40 mm, 10 mm, 5 mm, and  
68 1 mm and a vibration amplitude of 1 mm  
69 for 5 minutes.

### 70 **2.3. Feeding system**

71 Each fraction of ECs was then separately  
72 loaded into a custom conical bowl feeder  
73 (50 cm larger base diameter, 30 cm  
74 smaller base diameter, and 20 cm height).  
75 The vibration frequency was set up at the  
76 harmonic frequency of the bowl for the  
77 entire study (55.2 Hz). The amplitude of  
78 the vibration is controlled by the input  
79 voltage delivered by the controller  
80 (Variable Frequency Vibratory Feeder  
81 Controller SDVC31-M by Nanjing CUH  
82 Science and Technology Co., Ltd) and  
83 tuned for each EC size to optimise the  
84 feeding rate. The tension delivered was set  
85 at 110 V for components between 10 mm  
86 and 40 mm in size and 95 V for  
87 components with a size between 5 mm  
88 and 10 mm and 90 V for components with  
89 a size between 1 mm and 5 mm. These

1 parameters were determined through an  
2 empirical investigation for consistent  
3 feeding of the ECs at a rate of 2 ECs/s. A  
4 home-made passive rotary feeder was  
5 installed at the exit of the bowl feeder to  
6 ensure that the ECs were dispensed one at  
7 a time onto the conveyor belt.

#### 8 **2.4. Conveyor system**

9 The ECs were conveyed on a custom-  
10 made 10 cm width and 2.5 m long belt  
11 mounted on a 90 cm high aluminium  
12 frame. The belt speed was controlled by  
13 adjusting the rotational speed of a DC  
14 motor. In this study, the rotational speed  
15 of the motor was set to 100 rpm for the  
16 optical sorting and 57 rpm for MEXRT  
17 sorting, which corresponds to a linear  
18 speed of 26.3 cm/s and 15 cm/s,  
19 respectively, for ECs placed on the belt  
20 (Figure 1).

#### 21 **2.5. Vision system**

22 Images of ECs were acquired using a  
23 BU505MCF Telicam, Toshiba camera  
24 coupled with a white LED ring (V2DR-  
25 i90A-W, Vital Vision Technology).  
26 Database of ECs pictures was built using  
27 manually sorted components from  
28 WPCBs only used for the training of the  
29 CNN. This database of 3720 images  
30 divided into 8 classes of ECs was then  
31 used to train the CNN used for the ECs'  
32 images classification during the sorting  
33 process. Additionally, the dataset was  
34 augmented by applying random  
35 transformations such as rotation, flipping,  
36 and cropping to increase the size of the  
37 dataset and improve the generalization  
38 ability of the model. 70% of the database  
39 was used for the training of the model  
40 while 30% was used for the validation of  
41 the trained model. The CNN was coded in  
42 python (version 3.6.8) using the open-  
43 source library TensorFlow and the keras  
44 module. The CNN used in this study was  
45 a custom implementation based on a

46 sequential architecture with three 2D  
47 convolution blocks (with respectively 64,  
48 128, 256 output filters) each of them  
49 coupled with a max pool layer to reduce  
50 the output volume.

#### 51 **2.6. Multi energy X-ray** 52 **transmission sorting**

53 ECs placed on the conveyor belt were  
54 forced to pass in between the X-ray  
55 generator, (VJ X-RAY (NY) LLC  
56 MODEL: IXS160BP200P107 with  
57 tungsten anode, running at 100 kV and  
58 0.3 mA), and the MEXRT detector  
59 (ME100, Detection Technology). The  
60 latter was composed of a 128 pixels line  
61 each having an acquisition range from  
62 19.2 keV up to 160 keV with a 1.1 keV  
63 binning. Both source-sample and sample-  
64 detector distances were 10 cm. For each  
65 sample, 50 lines of pixels were acquired  
66 on the fly (while the EC was passing  
67 above the detector thanks to the  
68 conveyor's movement), with an  
69 acquisition time of 2 ms per line (which is  
70 maximum exposure time that would not  
71 cause the detector to become saturated  
72 while the generator was operating at its  
73 defined energy level), thus creating a  
74 hyperspectral 3D image of the EC. To get  
75 an image with as little distortion as  
76 possible, the conveyor speed was set to  
77 15 cm/s. It should be noted that to reduce  
78 the data collection size, the acquisition of  
79 the MEXRT detector was triggered by the  
80 detection of an EC by the upstream optical  
81 camera.

#### 82 **2.7. Data treatment**

83 For each pixel of the hyperspectral image,  
84 the total number of photons was integrated,  
85 giving a 2D grey scale image representing  
86 the X-ray transmission of the ECs. The  
87 pixel with the lowest photon count was  
88 considered as being part of the EC and a  
89 3\*3 square of pixels was extracted around  
90 it to conduct the elemental

1 characterisation. The  $k^{\text{th}}$  component of the  
2 average spectrum  $X \in \mathbb{N}^{128}$  was  
3 calculated from the chosen pixels as  
4 follow:

$$X_k = \frac{\sum_{i=1}^n \sum_{j=1}^n x_{i,j,k}}{n^2} \quad (1)$$

5 With  $x_{i,j,k} \in \mathbb{N}$  the  $k^{\text{th}}$  components of the  
6  $X_{i,j} \in \mathbb{N}^{128}$  spectrum corresponding to the  
7 pixel  $p_{i,j}$  and  $n$  the number of pixels of  
8 the studied area (hence, with the region of  
9 interest of size  $3 \times 3$  pixels used in this  
10 study, the sample size  $n$  is equal to 3).

11 The average spectrum was then filtered  
12 using the Savitzky-Golay filter (Python  
13 SciPy library, window length = 11,  
14 polynomial order = 3) to reduce noise. In  
15 X-ray spectrometry, the k-edge energy is a  
16 crucial parameter, representing the energy  
17 required for an electron to transition from  
18 a core level to an empty state in the

19 conduction band. This leads to a sharp  
20 increase in the photons absorption,  
21 resulting in a characteristic peak in the  
22 spectrum. By comparing this peak's  
23 energy with known k-edge energies of  
24 different elements, we can identify their  
25 presence. Local maxima of the spectra  
26 were extracted and compared with the k-  
27 edge values of the different elements  
28 studied with an error of  $\pm 1.1$  keV, to take  
29 into account the binning effect, which  
30 allows the differentiation of elements  
31 whose k-edges are separated by 1.1 keV.

## 32 **2.8. Pneumatic sorting system**

33 Once classified, ECs were ejected by  
34 pneumatic nozzles (KNS-R02-100-4 used  
35 with compressed azote - 6 bar) from the  
36 belt in different bins placed along the  
37 conveyor belt. Solenoid valves (VQ21A1-  
38 5GZ-C6-F) were controlled using the  
39 nidaqmx python library.

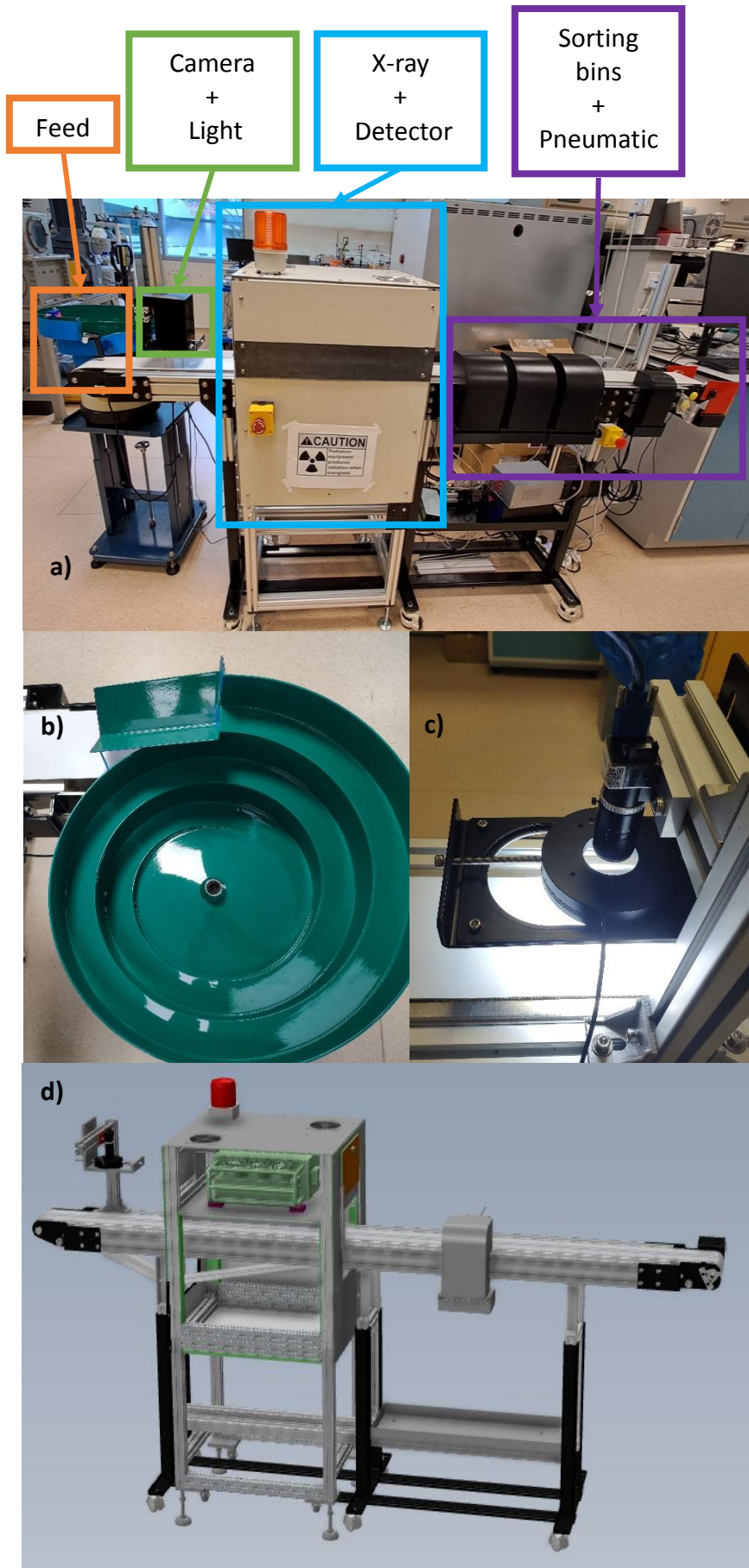


Figure 1: a) Photograph of the whole prototype, close view of the bowl feeder, c) close view of the camera and light and d) 3D CAD view of the prototype

## 2.9. Sample characterisation

**Sample preparation:** Each type of sorted electronic component was shredded separately using a cutting mill (Retsch SM200) with a built-in screen with 2 mm square side holes. The shredded particles were then subjected to either a grinder (Retsch RS200) if they were grindable, or a sample divider (Retsch PT100+DR100) if they contained ductile materials to further increase the compositional homogeneity

**XRF analysis:** To identify the different elements present in the sorted ECs, a first characterisation of the powder was done using X-ray fluorescence analysis (XRF). The powder prepared was then analysed using Vanta C series, Olympus XRF detector (soil method using 3 beams 15 kV, 40 kV and 50 kV).

**ICP-OES analysis:** Samples were analysed by Inductively Coupled Plasma-Optical Emission Spectrometry (ICP-OES). The samples were weighted (~0.20 g) and digested in a mixture of aqua regia (10 ml) and hydrogen peroxide (3 %, 2 ml) at 180 °C for 1 h using a microwave digestion system (ETHOS UP, MILESTONE). Metal contents in the digested solutions were measured with an ICP-OES spectrometer, (OP Optima 8000, PerkinElmer) after adequate dilution. Duplicate samples were prepared for each category and each sample was measured by ICP-OES in triplicate so that the mean values could be reported. Standard deviations were estimated by error propagation.

## 3. Results and discussion

The cornerstone of the shift in process paradigm is to start by a disassembly of the WPCBs, instead of their direct grinding to obtain free spent ECs. As there are many different disassembly processes available at the pre-industrial or even industrial level, which we recently reviewed (Maurice et al. 2021), we did not investigate this step further and emulated the “heating + shaking” method whenever necessary, following the method described in the part 2.1

### 3.1. Sieving

The first step in the sorting process was to separate the disassembled ECs into five size categories using sieves with apertures of 40 mm, 10 mm, 5 mm, and 1 mm. This enabled for a first physical classification of the components, hence reducing the diversity of the initial streams and facilitating the subsequent steps of the process. ECs larger than 40 mm were mainly connectors, while those smaller than 1 mm were typically tiny multilayer ceramic capacitors (MLCCs), resistors or broken parts or solder particles from the disassembly process. This smallest fraction represented less than 1 wt% of the total components (Figure 2). In addition, the MEXRT detector has a resolution of 0.8 mm, making it difficult to detect and analyze such small components (<1 mm) with the current geometry. A possible solution to tackle this issue is to use magnification by using a fan-shaped X-ray beam and increasing the distance between the sample and the detector. After manually dismantling twelve different WPCBs and counting the different ECs, the average weight of a component was found to be 24.67 g, 9.12 g, 0.83 g, 0.12 g, 0.006 g for the ECs with a size above 40 mm, 40 to 10 mm, 10 to 5 mm, 5 to 1 mm and less than 1 mm respectively.

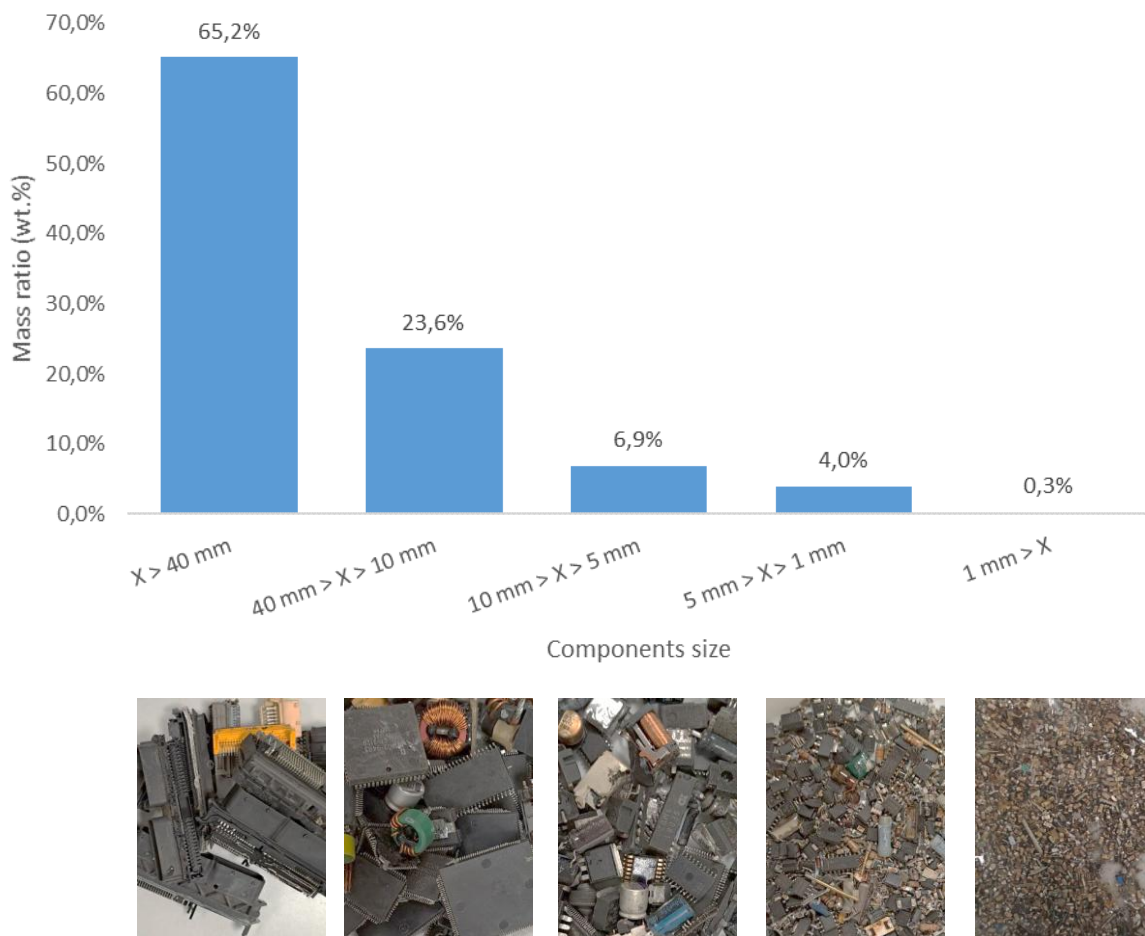


Figure 2: Mass distribution of the components in different size sub-fractions and their corresponding pictures

1 Given these limitations, the subsequent  
 2 sorting steps performed in this study  
 3 focused on the three fractions of ECs with  
 4 sizes comprised between 1 and 40 mm.  
 5 Overall, the results of the sieving step  
 6 showed that the system was able to  
 7 efficiently and accurately separate the ECs  
 8 into these different size categories, with  
 9 35 wt.% of the components falling within  
 10 the target size range for further analysis.  
 11 Fourteen different types of ECs with  
 12 chemical compositions of interest were  
 13 identified as the most common, of which,  
 14 between five to nine of them could be  
 15 found in the different size fractions,  
 16 therefore already significantly reducing  
 17 the heterogeneity of the ECs for the  
 18 subsequent sorting steps. The distribution  
 19 of the ECs by category can be

20 approximated by the average weight of an  
 21 EC for each category. In conclusion, the  
 22 sieving step of our sorting process is an  
 23 effective method and useful step for  
 24 separating electronic components into  
 25 different size categories. It allows for a  
 26 more targeted and efficient subsequent  
 27 sorting process, as the majority of the  
 28 components fall within the size range that  
 29 can be effectively classified. The quality  
 30 of the sieving step is critical to the success  
 31 of the subsequent sorting steps and to  
 32 improve the overall performance of the  
 33 sorting process.

34 **3.2. Process validation**

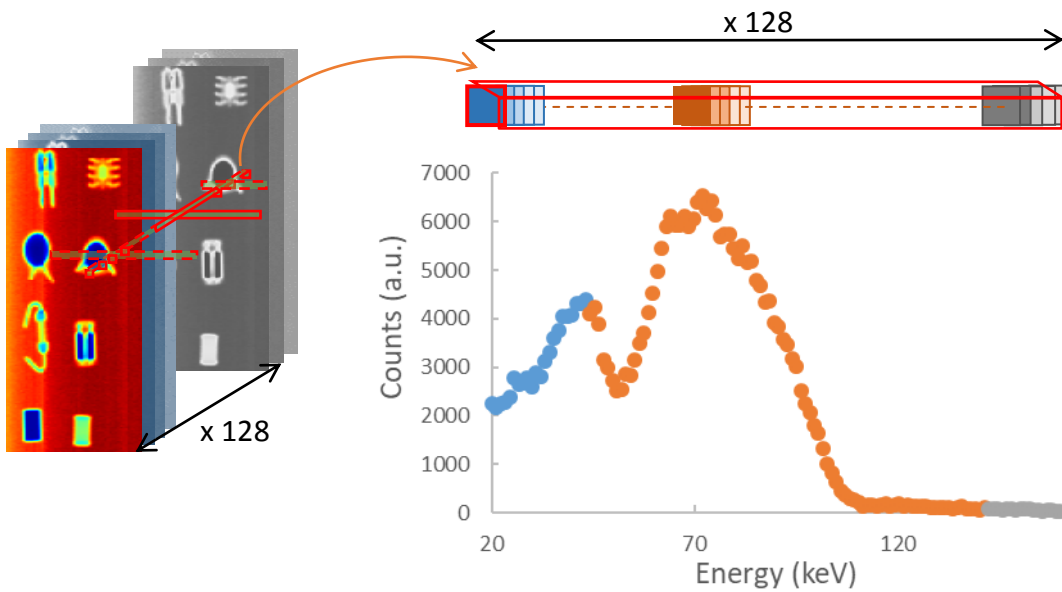
35 For the next sorting steps, we first  
 36 evaluated the performance of a sorting  
 37 approach consisting of an initial optical  
 38 sorting followed by MEXRT imaging. In  
 39 order to validate such a process and  
 40 evaluate its performance, a model sample  
 41 made of a controlled mixture of ECs was  
 42 prepared for each size sub-fraction.

43 Fourteen EC types were identified (Table  
 44 SI 1) as the most common found in PCBs,  
 45 which furthermore contained targeted  
 46 rarely recycled critical elements such as  
 47 Nd, Ta, Nb, Pd in capacitors, gold in  
 48 CPUs/connectors or aluminum in  
 49 electrolytic aluminum capacitors. IC chips  
 50 and connectors were treated together due  
 51 to their similar visual appearance and  
 52 elemental composition in the optical  
 53 classification step and sorted together.

a)

Stacking of 2D images

One pixel = 1 spectrum



b)

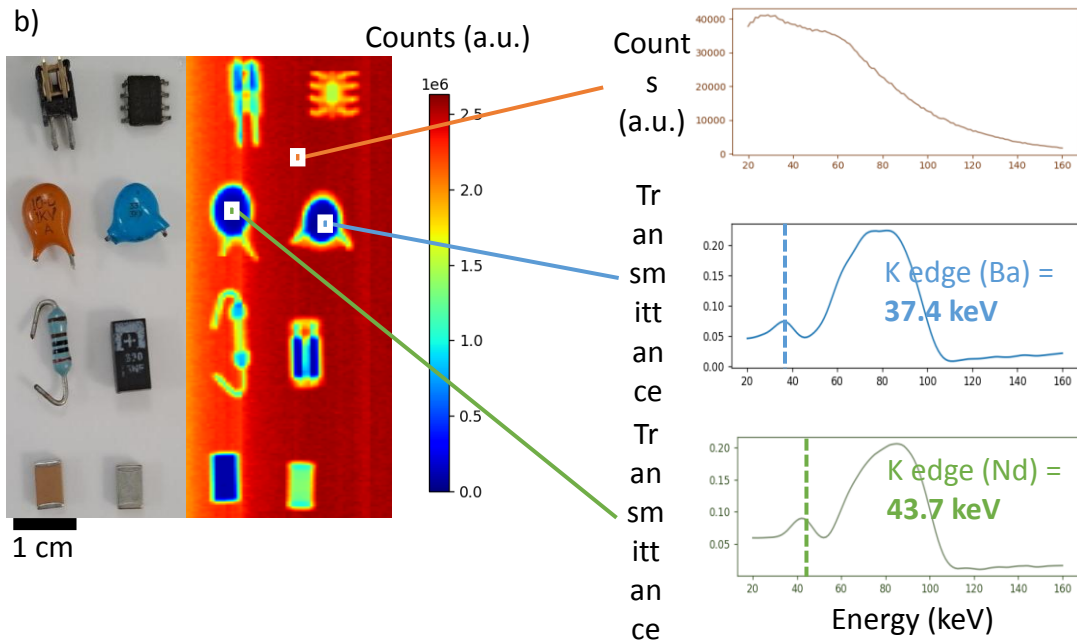


Figure 3: a) Spectra extraction from hyperspectral images and b) elements k-edge recognition.

1 The first sorting step based on optical  
2 sorting showed a global accuracy of  
3 97.4 % for a total of 8 categories (Table SI  
4 2, Table SI 3 and Table SI 4). The  
5 accuracy of the sorting process was  
6 evaluated by monitoring the number of  
7 ECs in the final bins, taking into account  
8 both the optical classification and the  
9 mechanical diversion of the different ECs  
10 into their respective sorting bins. With a  
11 minimum accuracy of 92.5 % for CPUs.  
12 This is to be compared to the current state  
13 of the art in optical sorting, which  
14 achieved a maximum of six EC categories  
15 with 98 % accuracy on their own training  
16 datasets, which could only give access to  
17 the most concentrated chemical  
18 elements(Lefkaditis and Tsirigotis 2010;  
19 Lu et al. 2022). By adding the MEXRT  
20 sorting step, which targets the k-edge of  
21 elements present in ECs (Figure 3), the  
22 system was able to separate optically  
23 similar components with different  
24 elemental compositions. The addition of

25 the MEXRT step gave a total sorting  
26 accuracy of the process to 96.9 %. By  
27 sorting the components using MEXRT  
28 and extracting the k-edge of known  
29 elements from the HSI (Figure 3),  
30 different categories of ceramic capacitors  
31 can be separated based on their elemental  
32 composition. This is the case for single  
33 layer capacitors (SLCC), which can be  
34 divided into 4 categories: barium-based  
35 SLCC, non-barium-based SLCC,  
36 neodymium-rich barium-based SLCC and  
37 tantalum capacitors (Figure 4). The same  
38 applies to MLCCs, which can be divided  
39 into two main categories: barium-based  
40 MLCCs and non-barium-based MLCCs.  
41 By using the transmittance of the ECs,  
42 XRT spectroscopy can easily separate  
43 relays from metallized polymer capacitors  
44 (MPCs) with 100 % precision which could  
45 not be done based solely on the ECs'  
46 features using optical sorting (Table SI 5,  
47 Table SI 6 and Table SI 7).

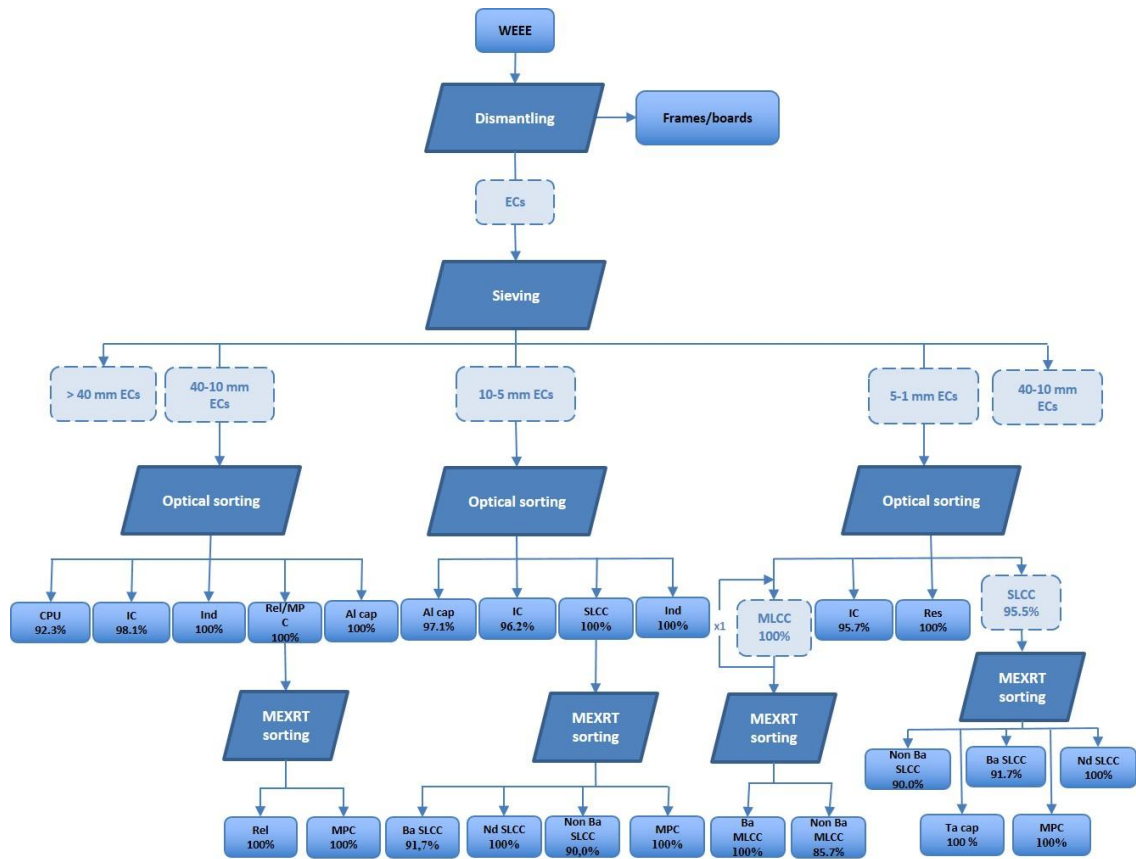


Figure 4: Flowchart of the sorting process for ECs

1 The optical sorting process can reach a  
 2 speed of 0.014 s/EC using a camera at a  
 3 speed of 75 frames per second. The  
 4 MEXRT acquisition speed used was 2 ms  
 5 per line acquired and 50 lines of 0.8 mm  
 6 were acquired for a total acquisition of 40  
 7 mm, resulting in a maximum sorting  
 8 speed of 0.1 s/EC. Considering the data  
 9 processing of the different images, with  
 10 the PC configuration used in this study,  
 11 the sorting speed for optical sorting was  
 12 reduced to 0.017 s/EC and 0.15 s/EC for  
 13 the MEXRT sorting (approximately  
 14 59 ECs/s and 7 ECs/s respectively). The  
 15 image pre-processing method efficiently  
 16 defines the region of interest using only a  
 17 minimum transmission finding, allowing  
 18 accurate EC localization even for low-  
 19 density materials, the only issue being the  
 20 detection of multiple ECs on the same  
 21 image, which is outside the scope of this  
 22 study. To ensure that consecutive  
 23 components are not too close to each other  
 24 during the MEXRT acquisition, a safety  
 25 distance corresponding to at least one

26 acquisition (100 ms) is left between the  
 27 components. This resulted in a maximum  
 28 speed of 0.25 s/EC for the MEXRT  
 29 sorting process. The average weight of an  
 30 EC was found to be 0.65 g, giving a  
 31 maximum average sorting speed of  
 32 9.36 kg/h. In real conditions, the sorting  
 33 speed was lowered to 0.5 s/EC (2 ECs/s)  
 34 to better control of the feeding system and  
 35 avoid stacking of components during  
 36 MEXRT sorting process. As a result, the  
 37 MEXRT process being significantly  
 38 slower than the optical sorting, it was  
 39 reserved for only a sub-fraction of the  
 40 total ECs for which an elemental based  
 41 sorting was required. Although the overall  
 42 accuracy may be slightly lower than the  
 43 pure optical method, MEXRT provides  
 44 the added advantage of being able to  
 45 differentiate similar-looking ECs with  
 46 different compositions without impacting  
 47 the high accuracy if the optical sorting.

48 In conclusion, our sorting process using  
 49 both optical sorting and X-ray

50 transmission techniques is a highly  
 51 effective method for accurately classifying  
 52 and separating electronic components. The  
 53 system has a high sorting accuracy and  
 54 speed, making it a valuable tool for  
 55 electronic component recycling.

### 56 3.3. Real samples sorting 57 process/Scalability study

58 The sorting process results were then  
 59 scaled-up to a larger batch of waste by  
 60 applying the same method to a mixture of  
 61 9056.5 g of printed circuit boards from  
 62 engine control units. After disassembly,  
 63 5409.4 g of ECs were recovered and  
 64 sieved for further sorting (Figure 5). Each  
 65 sorted fraction was shredded into  
 66 homogeneous powder and then analysed  
 67 by XRF for a first qualitative analysis of  
 68 the composition, followed by a  
 69 quantitative analysis of the target elements

70 by ICP-OES. The analysis of the sorted  
 71 ECs in the final streams showed a clear  
 72 enrichment of the target elements such as  
 73 gold, Al, Pd, Mn and Cu. The enrichment  
 74 of gold was found to be up to 0.14 wt.% in  
 75 CPUs while it was below the detection  
 76 limit in the reference mixture (below  
 77 0.1 ppm). This represents an increase of  
 78 four orders of magnitude in concentration.  
 79 It was also found to be up to 53.95 wt.%  
 80 for Al in electrolytic capacitors with a size  
 81 between 40 and 10 mm. The segregation  
 82 of the ECs does not only enrich the final  
 83 streams in certain elements but also  
 84 reduces the heterogeneity of some classes.  
 85 This is the case of the inductors sorting  
 86 bin (5-10 mm), which is composed of  
 87 45.6 wt.% of iron, 38.5 wt.% of copper  
 88 and 20.82 wt.% of tin with only traces  
 89 amounts of other metallic elements (Ni,  
 90 Zn, Al).

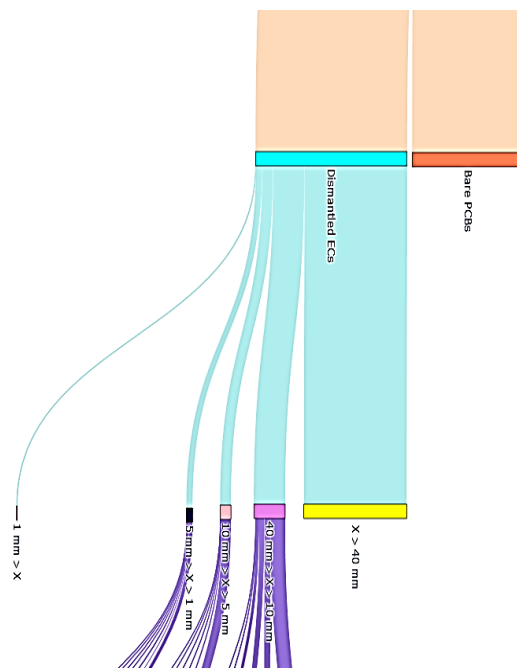


Figure 5: Mass flow diagram for the up-scaled process

1 From a global point of view of the overall  
 2 process, a convenient way to represent the  
 3 simplification that it allows for is to  
 4 compare the entropies of all the sorting  
 5 bins obtained, which can be estimated  
 6 using the Boltzmann equation:

$$7 \quad S = -k_B \sum_{i=1}^n x_i \log(x_i) \quad (2)$$

8 Where  $k_B$  the Boltzmann constant and  $x_i$   
 9 the mass ratio of the elements present in  
 10 the ECs measured by ICP-OES. The  
 11 results of this calculation are shown in  
 12 Figure 6-a. In the latter, one can compare

13 the entropy of each sorting bin with the  
14 entropy of the reference mixture of ECs  
15 plus the composition of a bare WPCB  
16 (Smalcerz et al. 2023). Any fraction with  
17 an entropy lower than the latter, can be  
18 said to have a simpler composition. This  
19 comparison shows that all fractions have a  
20 significantly lower entropy than the one of  
21 the ground WPCB. This reduction of the  
22 entropy of the phase is particularly visible  
23 for inductors and relays, which are mainly  
24 composed of iron and copper. In the cases  
25 with the highest entropy, such as the  
26 category labelled “5-1 mm other SLCC”,  
27 this level of entropy comes from the  
28 sorting induced enrichment in Mn, Zn and  
29 Bi, that are now no longer present in  
30 traces, and therefore significantly  
31 contribute to the entropy. Same goes for  
32 the MPCs sorting bin, which after sorting

33 contained up to 47.04 wt.% of tin (Table  
34 SI 8).

35 Overall, looking at Figure 6-b and  
36 comparing the number of major elements  
37 present either in the initial WPCB or in  
38 each of the sorting bins, it can be seen that  
39 all the sorted categories have much  
40 simpler composition, especially when  
41 only considering the number of major  
42 elements in their composition (all have  
43 less than six elements with concentration  
44 over 1 wt.%, to be compared to thirteen in  
45 the original WPCB). This demonstrates  
46 that the process is not only effective in  
47 separating and classifying electronic  
48 components, but it also easily and  
49 effectively concentrates valuable metals,  
50 thus facilitating subsequent chemical  
51 separation, a key requirement for making  
52 their recycling economically viable.

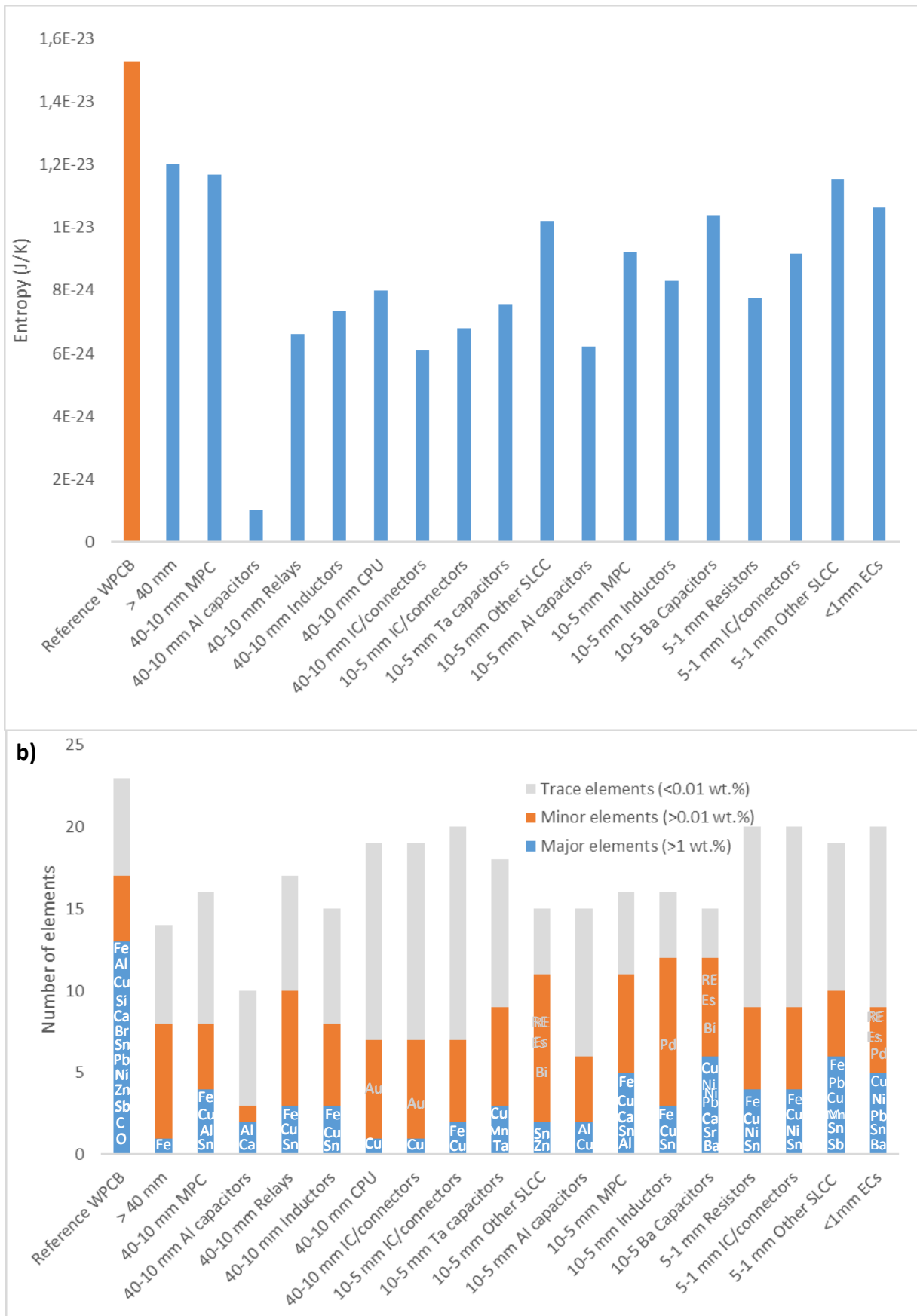


Figure 6: a) entropy of metals and b) number of elements in the different sorted categories. All chemical elements present in the major elements fraction (blue blocks) are listed in white. Significant elements that were either at trace level or below

*the detection limits (at WPCB level) but could be enriched during the process to the level of "Minor elements", are indicated in grey over the orange blocks.*

### **3.4. Throughput and process industrial implementation**

This sorting process presents a great opportunity for the development of economically viable processes. The viability of this process was previously reported by (Xia et al. 2022) in the study of neodymium from Nd-based SLCC. Although this study only considered the recovery of Nd-based SLCC, the process was already showing a payback time of less than 5 years. While other recycling processes targeting specific ECs have been developed (Chen et al. 2021; Niu and Xu 2018; Wang and Xu 2017), they often lacked a mean of obtaining concentrated streams of the targeted ECs. This sorting process addresses this issue by effectively classifying and separating ECs, allowing for the recovery of valuable materials in a concentrated form. The ability to recover these materials in a concentrated form significantly improves the economic viability of the recycling process. This technology has the potential to revolutionise the field of electronic waste management and recycling by providing an efficient and cost-effective method of recovering valuable materials from discarded electronic components. However, the limitations of the process lie in the in-line treatment of the ECs, and the sorting speed will be improved in further development of the prototype by using a parallel sorting. We developed a demonstrator at a laboratory scale to validate the feasibility of advanced sorting and its compatibility with industrial plants by testing the sorting capability as a function of belt speed, although a larger, multi-lane industrial sorting tool would use similar conveyor speed. The cost of the prototype was broken down as follows: 50,000 USD for the X-ray system (generator, detector, shielding), 2,500 USD for the control and data acquisition

systems, and 12,500 USD for the mechanical structure, conveyor belt and sorting system. It is important to note that the costs of a laboratory-scale prototype may not be directly transferable to a larger, multi-lane industrial sorting tool. On a 1 meter large conveyor belt, up to 50 ECs can be treated in parallel. Thus, the sorting speed of the prototype would be multiplied by fifty allowing the sorting of up to 500 kg/h. Considering that a country such as Singapore produces an average of 60000 tonnes of e-waste per year, resulting in approximately 1620 tonnes of ECs (PCBs represent 6 wt.% of the global e-waste (Pinho, Ferreira, and Almeida 2018)), 3240 machine hours would be required, equivalent to 125 days. Hence, this process shows promising results for industrialisation.

### **4. Conclusion**

In conclusion, our instrumental developments and integration reported here presents a highly effective sorting process for electronic components (ECs) that combines physical, optical and MEXRT-based tools and process steps. The overall process is capable of concentrating valuable chemical elements in the final streams with, for example, an enrichment of up to 10,000 times its initial content in the WPCBs in the case of gold, including metals that are currently wasted and not recovered in industrial recycling settings. Achieving such levels of enrichment, while combining high accuracy and low operating costs, opens up new opportunities in the recycling industry, especially regarding these elements that are lost in WEEE recycling processes. Indeed, such elementally enriched fractions can either be traded or purified by hydrometallurgy. In the latter case, one still has to face the issue of the variability of the composition of the sorting bags, which can be solved thanks to state of the art

microfluidics based rapid process development tools (Maurice et al. 2022; Olivier et al. 2022, 2023).

**Credit authorship contribution statement**

**Nicolas M. Charpentier:** Conceptualization, Methodology, Software, Investigation, Data curation & Interpretation, Writing- Original draft preparation. **Ange A. Maurice:** Conceptualization, Investigation, Reviewing and Editing. **Dong Xia:** Investigation, Data curation and Interpretation, Writing- Reviewing and Editing. **Wen-Jie Li:** Investigation. **Chang-Sian Chua:** Investigation. **Andrea Brambilla:** Conceptualization. **Jean-Christophe P. Gabriel:** Conceptualization, Methodology, Data Interpretation, Writing- Reviewing and Editing, Supervision, Funding acquisition, Project administration.

**Declaration of Competing Interest**

NMC and JCG wish to declare that MEXRT detector ME100 used in the work described here is commercialised by Detection Technology under patent licensing from CEA. The authors declare no other competing interests.

**Acknowledgement**

All authors acknowledge financial support from SCARCE project, which is supported by the National Research Foundation, Singapore, and the National Environment Agency, Singapore under its Closing the Waste Loop R&D Initiative (Award No. [USS-IF-2018-4](#)) and Closing the Resource Loop Funding Initiative (Award No. CTRL-2022-1D-01). NC acknowledges financial support (salary) in 2023 by the REVIWEEE project grant managed by the French National Research Agency (ANR) under the France 2030 programme, award No. [ANR-22-PERE-0009](#).

## References

- Binnemans, Koen, Paul McGuinness, and Peter Tom Jones. 2021. "Rare-Earth Recycling Needs Market Intervention." *Nature Reviews Materials* 6(6):459–61. doi: 10.1038/s41578-021-00308-w.
- Chen, Yao, Mengjiao Xu, Jieya Wen, Yu Wan, Qingfei Zhao, Xia Cao, Yong Ding, Zhong Lin Wang, Hexing Li, and Zhenfeng Bian. 2021. "Selective Recovery of Precious Metals through Photocatalysis." *Nature Sustainability* 4(7):618–26. doi: 10.1038/s41893-021-00697-4.
- Forti, Vanessa, Cornelis Peter Baldé, Ruediger Kuehr, and Garam Bel. 2020. *The Global E-Waste Monitor 2020*.
- Gorewoda, Tadeusz, Marcus Eschen, Jadwiga Charasińska, Magdalena Knapik, Sylwia Kozłowicz, Jacek Anyszkiewicz, Michał Jadwiński, Martyna Potempa, Marta Gawliczek, Andrzej Chmielarz, and Witold Kurylak. 2020. "Determination of Metals' Content in Components Mounted on Printed Circuit Boards from End-of-Life Mobile Phones." *Recycling* 5(3):1–9. doi: 10.3390/recycling5030020.
- Hennebert, Pierre, and Montserrat Filella. 2018. "WEEE Plastic Sorting for Bromine Essential to Enforce EU Regulation." *Waste Management* 71:390–99. doi: 10.1016/j.wasman.2017.09.031.
- Kaya, Muammer. 2017. "Recovery of Metals and Nonmetals from Waste Printed Circuit Boards (PCBs) by Physical Recycling Techniques." Pp. 433–51 in *Minerals, Metals and Materials Series*. Springer International Publishing.
- Kopacek, Bernd. 2016. "Intelligent Disassembly of Components from Printed Circuit Boards to Enable Re-Use and More Efficient Recovery of Critical Metals." *IFAC-PapersOnLine* 49(29):190–95. doi: 10.1016/j.ifacol.2016.11.100.
- Lefkaditis, D., and G. Tsigotis. 2010. "Intelligent Optical Classification System for Electronic Components." *Elektronika Ir Elektrotechnika* (2):10–14. doi: 10.5755/j01.eee.98.2.9914.
- Lu, Yingqi, Bo Yang, Yichun Gao, and Zhenming Xu. 2022. "An Automatic Sorting System for Electronic Components Detached from Waste Printed Circuit Boards." *Waste Management* 137(July 2021):1–8. doi: 10.1016/j.wasman.2021.10.016.
- Maurice, Ange A., Khang Ngoc Dinh, Nicolas M. Charpentier, Andrea Brambilla, and Jean Christophe P. Gabriel. 2021. "Dismantling of Printed Circuit Boards Enabling Electronic Components Sorting and Their Subsequent Treatment Open Improved Elemental Sustainability Opportunities." *Sustainability (Switzerland)* 13(18). doi: 10.3390/su131810357.
- Maurice, Ange A., Johannes Theisen, Varun Rai, Fabien Olivier, Asmae El Maangar, Jean Duhamet, Thomas Zemb, and Jean - Christophe P. Gabriel. 2022. "First Online X - ray Fluorescence Characterization of Liquid - liquid Extraction in Microfluidics." *Nano Select* 3(2):425–36. doi: 10.1002/nano.202100133.
- Mesina, M. B., T. P. R. de Jong, and W. L. Dalmijn. 2007. "Automatic Sorting of Scrap Metals with a Combined Electromagnetic and Dual Energy X-Ray Transmission Sensor." *International Journal of Mineral Processing* 82(4):222–32. doi: 10.1016/j.minpro.2006.10.006.
- Niu, Bo, and Zhenming Xu. 2018. "From Waste Metallized Film Capacitors to Valuable Materials: Hexagonal Flake-Like Micron Zinc Powder, Copper-Iron Electrodes, and an Energy Resource." *ACS Sustainable Chemistry and Engineering* 6(9):12281–90. doi: 10.1021/acssuschemeng.8b02702.
- Olivier, Fabien L., Sarah M. Chevrier, Barbara Keller, and Jean Christophe P. Gabriel. 2023. "On-Line Quantification of Solid-Phase Metal Extraction Efficiencies Using Instrumented Millifluidics Platform." *Chemical Engineering Journal* 454(P3):140306. doi: 10.1016/j.cej.2022.140306.
- Olivier, Fabien, Ange A. Maurice, Daniel Meyer, and Jean Christophe Gabriel. 2022. "Liquid-Liquid Extraction: Thermodynamics-Kinetics Driven Processes Explored by Microfluidics." *Comptes Rendus Chimie* 25:137–48. doi: 10.5802/crchim.172.
- Pinho, Sílvia, Marco Ferreira, and Manuel F. Almeida. 2018. "A Wet Dismantling Process for the Recycling of Computer Printed Circuit Boards." *Resources, Conservation and Recycling* 132(January):71–76. doi: 10.1016/j.resconrec.2018.01.022.

- Rapolti, Laszlo, Holonec Rodica, Laura Grindei, Marius Purcar, Florin Dragan, Romul Copîndean, and Robert Reman. 2021. "Experimental Stand for Sorting Components Dismantled from Printed Circuit Boards." *Minerals* 11(11). doi: 10.3390/min11111292.
- Sauer, Florian, Bum Ki Choi, Gesa Beck, and Mathias Wickleder. 2019. "Recovery of Tantalum from Printed Circuit Boards: An Overview of the IRETA Project." *World of Metallurgy - ERZMETALL* 72(4):216–22.
- Shakil, Sidra, Khazeema Nawaz, and Yumna Sadeq. 2023. "Evaluation and Environmental Risk Assessment of Heavy Metals in the Soil Released from E-Waste Management Activities in Lahore, Pakistan." *Environmental Monitoring and Assessment* 195(1). doi: 10.1007/s10661-022-10701-9.
- Smalcerz, Albert, Tomasz Matula, Michal Slusorz, Julia Wojtasik, Weronika Chaberska, Szymon Kluska, Lukasz Kortyka, Lukasz Mycka, Leszek Blacha, and Jerzy Labaj. 2023. "The Use of PCB Scrap in the Reduction in Metallurgical Copper Slags." *Materials* 16(2):1–15. doi: 10.3390/ma16020625.
- Tan, Wenjie, Qinyuan Duan, Linpeng Yao, and Jia Li. 2022. "A Sensor Combination Based Automatic Sorting System for Waste Washing Machine Parts." *Resources, Conservation and Recycling* 181(March):106270. doi: 10.1016/j.resconrec.2022.106270.
- U.S. Environmental Protection Agency, Office, and of Resource Conservation. 2020. "Documentation for Greenhouse Gas Emission and Energy nicolas Used in the Waste Reduction Model (WARM) Electronics." (November).
- Veras, Moacir Medeiros, Aaron Samuel Young, Cristiano Rocha Born, Artur Szewczuk, Artur Cezar Bastos Neto, Carlos Otávio Petter, and Carlos Hoffmann Sampaio. 2020. "Affinity of Dual Energy X-Ray Transmission Sensors on Minerals Bearing Heavy Rare Earth Elements." *Minerals Engineering* 147(November 2019). doi: 10.1016/j.mineng.2019.106151.
- Wang, Jianbo, and Zhenming Xu. 2015. "Disposing and Recycling Waste Printed Circuit Boards: Disconnecting, Resource Recovery, and Pollution Control." *Environmental Science and Technology* 49(2):721–33. doi: 10.1021/es504833y.
- Wang, Jianbo, and Zhenming Xu. 2017. "Environmental Friendly Technology for Aluminum Electrolytic Capacitors Recycling from Waste Printed Circuit Boards." *Journal of Hazardous Materials* 326:1–9. doi: 10.1016/j.jhazmat.2016.10.039.
- Wu, Zebing, Wenyi Yuan, Jinhui Li, Xiaoyan Wang, Lili Liu, and Jingwei Wang. 2017. "A Critical Review on the Recycling of Copper and Precious Metals from Waste Printed Circuit Boards Using Hydrometallurgy." *Frontiers of Environmental Science and Engineering* 11(5). doi: 10.1007/s11783-017-0995-6.
- Xia, Dong, Nicolas M. Charpentier, Ange A. Maurice, Andrea Brambilla, Qingyu Yan, and Jean Christophe P. Gabriel. 2022. "Sustainable Route for Nd Recycling from Waste Electronic Components Featured with Unique Element-Specific Sorting Enabling Simplified Hydrometallurgy." *Chemical Engineering Journal* 441(March):135886. doi: 10.1016/j.cej.2022.135886.
- Yeyu, Y., J. Wenbao, H. Daqian, S. Aiyun, C. Can, Q. Mengcheng, Z. Gangqiang, J. Limin, and T. Yajun. 2021. "Feasibility Study of a Method for Identification and Classification of Magnesium and Aluminum with ME-XRT." *Journal of Instrumentation* 16(11). doi: 10.1088/1748-0221/16/11/P11041.
- Zeng, Qiang, Jean Baptiste Sirven, Jean Christophe P. Gabriel, Chor Yong Tay, and Jong Min Lee. 2021. "Laser Induced Breakdown Spectroscopy for Plastic Analysis." *TrAC - Trends in Analytical Chemistry* 140:116280. doi: 10.1016/j.trac.2021.116280.